11th World Congress on Computational Mechanics (WCCM XI)
5th European Conference on Computational Mechanics (ECCM V)
6th European Conference on Computational Fluid Dynamics (ECFD VI)
E. Oñate, J. Oliver and A. Huerta (Eds)

ON THE WAKE TRANSITION IN THE FLOW PAST A CIRCULAR CYLINDER AT CRITICAL REYNOLDS NUMBERS

Ivette Rodríguez[1], Oriol Lehmkuhl[1,2] Jorge Chiva[1], Ricard Borrell[1,2] and Assensi Oliva[1]

[1] Heat and Mass Transfer Technological Center (CTTC), Universitat Politècnica de Catalunya-BarcelonaTech (UPC). Colom 11, 08222 Terrassa (Barcelona), cttc@cttc.upc.edu
[2] Termo Fluids, S.L. Av. Jaquard, 97 1-E, 08222 Terrassa (Barcelona), Spain. termofluids@termofluids.com

Key words: drag crisis, wake topology, unsteady forces, vortex shedding

Abstract. In this paper advanced turbulence simulations at Reynolds numbers in the range of 1.4×10^5-8.5×10^5 will be carried out by means of large-eddy simulations. Numerical simulations using unstructured grids up to 90 million of control volumes have been performed on Marenostrum Supercomputer. One of the major outcomes of this work is to shed some light on the wake topology and flow features at critical and supercritical Reynolds numbers, whilst at the same time to study the shear layer instabilities mechanisms and their role on the drag crisis phenomena.

1 INTRODUCTION

The flow past a circular cylinder is a canonical case which is of relevance for many practical applications. This case has been extensively studied both experimentally (see for instance [1, 2]) and numerically (e.g. [3, 4]). In spite of its simple geometry, the presence of interesting flow features continues to make this problem subject of many current studies. This problem is characterised by flow separations, transition to turbulence in the separated shear layer and, the shedding of vortices. Williamson in its review [5], performed a comprehensive description of the different flow phenomena and regimes at different Reynolds numbers. Steady laminar flow exists at Reynolds numbers up to approximately 40 (based on the cylinder diameter and the free-stream velocity) with a pair of steady dipole vortices forming behind the cylinder. The laminar vortex shedding, also known as the von-Kármán vortex street, is observed at Reynolds numbers up to about 190. When the Reynolds number is approximately 260, the flow experiences a transition to a three dimensional finer scale. With increasing Reynolds number, the three dimensional cylinder wake becomes more chaotic. Finally, at Reynolds number around

1200 the shear layers separating from the cylinder become unstable[6]. As the Reynolds numbers approaches a critical value around 2×10^5, the transition to turbulence moves towards the cylinder surface causing the delaying of the separation point and a dramatic decrease of the drag force on the cylinder surface. In the critical Reynolds number range ($Re = 2 \times 10^5$ - 3.5×10^5), flow transition is accompanied of different regimes such as the presence of asymmetric forces on the cylinder surface, which cause average lift to be greater than zero [7, 8]. At higher Reynolds numbers, beyond 3.5×10^6, the boundary layer at the cylinder becomes turbulent before separation (see for instance [1]).

In the range $2 \times 10^5 < Re < 5 \times 10^5$, also known as the critical regime[9, 10, 8] there is a sharp decrease of the drag coefficient magnitude, falling to a minimum value of $C_D \approx 0.2$. In this regime, transition to turbulence firsts occurs in one of the boundary layers and is characterised by a separation with further reattachment of the boundary layer, forming a bubble similar to that observed in the flow past airfoils at low-to-moderate Reynolds numbers. This laminar separation bubble (LSB) on one side of the cylinder surface is the cause of asymmetric forces acting on the cylinder surface with a mean lift coefficient greater than zero ($C_L > 0$). Flow separation in the transitional shear-layers occurs further downstream at about 140° (measured from the front stagnation point). Once the drag coefficient reaches its minimum value, (i.e. supercritical regime with $Re = 5 \times 10^5 - 2 \times 10^6$), two LSB on both sides of the cylinder surface are established citeDEL53-TR,ACH68-A,SHI93-A. In this regime, the wake is thinner with width lower than the cylinder diameter. There is much controversy about whether vortex shedding exists or it is completely suppressed [8, 11]. In this work large-eddy simulations of the flow at critical and super-critical Reynolds numbers in the range of $Re = U_{ref}\ D/\nu = 1.4 \times 10^5\ -\ 8.5 \times 10^5$ are carried out. This aims at shedding some light into the changes in topology which occur at these Reynolds numbers and to answer the question whether vortex shedding is suppressed at supercritical Reynolds numbers.

2 MATHEMATICAL AND NUMERICAL MODEL

2.1 Governing equations

The spatially filtered Navier-Stokes equations can be written as,

$$\frac{\partial \overline{u}_i}{\partial t} = 0 \tag{1}$$

$$\frac{\partial \overline{u}_i}{\partial t} + \frac{\partial \overline{u}_i \overline{u}_j}{\partial x_j} - \nu \frac{\partial^2 \overline{u}_i}{\partial x_j \partial x_j} + \rho^{-1} \frac{\partial \overline{p}}{\partial x_i} = -\frac{\partial \mathcal{T}_{ij}}{\partial x_j} \tag{2}$$

where $\overline{u}$ and $\overline{p}$ stand for the filtered velocity and pressure, respectively. ν is the kinematic viscosity and ρ the density of the fluid. In the equation 2, $\mathcal{T}_{ij}$ is the subgrid scale (SGS) stress tensor which has to be modeled. Its deviatoric part is given by,

$$\mathcal{T}_{ij} - \frac{1}{3}\mathcal{T}_{kk}\delta_{ij} = -2\nu_{sgs}\overline{\mathcal{S}}_{ij} \tag{3}$$

where $\overline{\mathcal{S}}_{ij}$ is the large-scale rate-of-strain tensor, $\overline{\mathcal{S}}_{ij} = \frac{1}{2}\left(g_{ij} + g_{ji}\right)$ being $g_{ij} = \partial\overline{u}_i/\partial x_j$. δ_{ij} is the Kronecker delta. To close the formulation, an appropriate expression for the subgrid-scale viscosity should be provided. In this paper, the wall-adapting local-eddy viscosity model (WALE) [12] is used. This model, proposed by Nicaud and Ducros [12] evaluates the eddy viscosity using the square of the velocity gradient tensor. In its formulation, the SGS viscosity accounts for the effects of both the strain and the rotation rates of the smallest resolved turbulent fluctuations. In addition, it has a proper near-wall behavior ($\nu_{sgs} \propto y^3$). The WALE model evaluates the eddy viscosity as,

$$\nu_{sgs} = (\mathcal{C}_w\Delta)^2 \frac{(\overline{\mathcal{V}_{ij}} : \overline{\mathcal{V}_{ij}})^{\frac{3}{2}}}{(\overline{\mathcal{S}_{ij}} : \overline{\mathcal{S}_{ij}})^{\frac{5}{2}} + (\overline{\mathcal{V}_{ij}} : \overline{\mathcal{V}_{ij}})^{\frac{5}{4}}} \tag{4}$$

in the above expression, $\overline{\mathcal{V}_{ij}}$ is the deviatoric part of the square of the velocity gradient tensor $\overline{\mathcal{V}_{ij}} = \frac{1}{2}\left(g_{ij}^2 + g_{ji}^2\right) - \frac{1}{3}\delta_{ij}g_{kk}^2$ with $g_{ij}^2 = g_{ik}g_{kj}$. $\mathcal{C}_w$ is the model constant, here a value of $\mathcal{C}_w = 0.325$ is used.

2.2 Numerical method

The governing equations have been discretized on a collocated unstructured grid arrangement by means of second-order spectra-consistent schemes [13]. Such schemes are conservative, i.e. they preserve the symmetry properties of the continuous differential operators and, ensure both stability and conservation of the kinetic-energy balance even at high Reynolds numbers and with coarse grids. For the temporal discretization of the momentum equation (2) a two-step linear explicit scheme on a fractional-step method has been used for the convective and diffusive terms [14], while for the pressure gradient term an implicit first-order scheme has been implemented. This methodology has been previously used with accurate results for solving the flow over bluff bodies with massive separation [15, 16, 4, 17].

2.3 Definition of the case and boundary conditions

The flow past a circular cylinder at critical and super-critical Reynolds numbers in the range of $Re = U_{ref}\,D/\nu = 1.4\times10^5 - 8.5\times10^5$ is considered. The Reynolds number is defined in terms of the free-stream velocity U_{ref} and the cylinder diameter D. The cases are solved in a computational domain of dimensions $x \equiv [-16D, 16D]$; $y \equiv [-10D, 10D]$; $z \equiv [0, 0.5\pi D]$ in the stream-, cross- and span-wise directions respectively, with a circular cylinder at (0,0,0). The boundary conditions at the inflow consist of uniform velocity (u,v,w)=(1,0,0), slip conditions at the top and bottom boundaries of the domain, while at the outlet a pressure-based condition is used. At the cylinder surface, no-slip conditions are prescribed. As for the span-wise direction, periodic boundary conditions are imposed.

Different grids up to ~ 90 million CVs are used, depending on the Reynolds number. The boundary layer at the cylinder surface is well resolved, i.e. no wall function is used. Thus, the meshes are designed so as to keep the non-dimensional wall distance $y^+ \leq 2$.

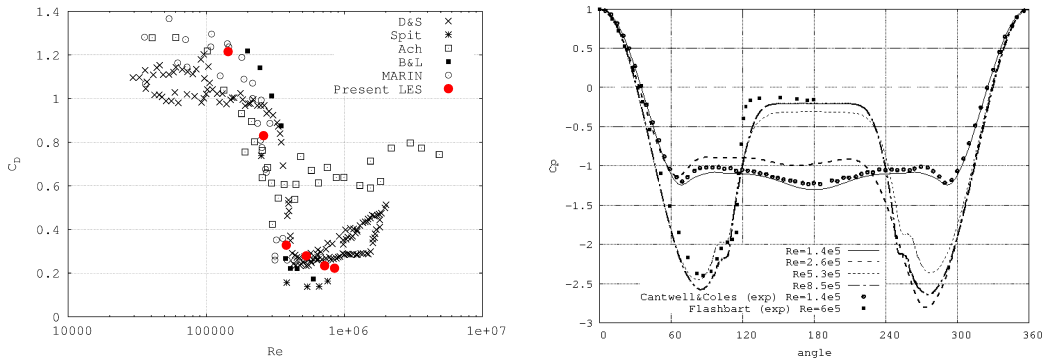

(a) (b)

Figure 1: (left)Drag coefficient vs. Reynolds number. (right) Pressure coefficient on the cylinder surface

To do this, a prism layer is constructed around the cylinder surface. In the problem here considered, transition to turbulence occurs in the boundary layer. Thus, it should be stressed that in the present formulation transition to turbulence is well captured by the model, i.e. no artificial mechanism is imposed for triggering this phenomenon to occur.

3 RESULTS

The simulations have been started from homogeneous flow and initially some random perturbations have been introduced. In order to ensure a temporal converged statistically steady state, the flow field has been advanced in time until the initial transient has been washed out. Then, statistics have been collected and averaged over approximately 25 shedding cycles.

Figure 1 depicts the total drag coefficient and the pressure distribution on the cylinder surface at different Reynolds numbers compared with experimental results from the literature. At these Reynolds numbers, there is a large scattering in the measurements, as this quantity is highly affected by the cylinder surface roughness, wind tunnel blockage ratio, inlet conditions, etc., making difficult measurements at this range of Reynolds numbers. Nonetheless, there is a reasonable agreement between numerical and experiment results for the whole range of Reynolds numbers considered. The main flow parameters are summarised in Table 1.

As the Reynolds numbers comes closer to the critical regime, the location of the separation of the shear layers moves towards the cylinder rear end. In fact, at $Re = 1.4 \times 10^5$, it occurs at $\theta = 95°$ which is in good agreement with the value reported by [18] of $\theta = 94°$. With the increase in the Reynolds number up to 2.5×10^5 (upper critical range), the transition to turbulence is earlier triggered on one side of the cylinder. This causes an asymmetry in the forces acting on the cylinder surface (see figure 1(b) at $Re = 2.5 \times 10^5$) and a non-zero magnitude of the lift coefficient $C_l > 0$. As a consequence, separation is delayed in the turbulent side, it occurs at about $\theta = 108°$, whereas at the other shear

Re	C_D	$-Cp_b$	$\varphi_{sep}[^\circ]$	$\varphi_{Pmin}[^\circ]$	St
1.4×10^5	1.215	1.3	95.5	68.5	0.21
2.5×10^5	0.83	0.984	95/252	70/280	0.238
3.8×10^5	0.46	0.347	102	83.8	0.238/0.355
5.3×10^5	0.296	0.303	101	82	0.368
7.2×10^5	0.233	0.224	102.81	84	0.449
8.5×10^5	0.216	0.209	103.6	84.2	0.459

Table 1: Flow parameters at different Re numbers. C_D drag coefficient, Cp_b base pressure, φ_{sep} separation angle (for the cases with LSB indicates the location of the first separation),φ_{Pmin} location where minimum pressure occurs, St vortex shedding frequency.

layer the flow still separates at $\theta = 95^\circ$ as can readily be observed in figure 2(a). This behaviour, was also reported experimentally by Bearman [10] and Schewe [8]. With the further increase in the Reynolds number, a second bubble appears on the other side of the cylinder, but the flow is still asymmetric ($Re = 3.8 \times 10^5$). At $Re = 5.3 \times 10^5$, symmetry is almost recovered and, as the drag approaches to its minimum value $Re = 7.2 \times 10^5$ the wake also becomes narrow (see also figure 2).

There is little information about the vortex shedding in the range of critical-supercritical regime, contrary to the subcritical regime, where consistent measurements of this quantity can be found and there is an agreement about the non-dimensional vortex shedding frequency $St = fU/D =\sim 0.19 - 0.21$. At these Reynolds numbers, values reported are quite scattered and inconsistency in the measurements are found. In fact, it has been argued that in the super-critical regime vortex shedding ceases to occur (see for instance [11]). However, in the present computations vortex shedding does occur at every Reynolds number. Indeed, in the critical regime Strouhal number increased from 0.21 to 0.36 at $Re = 5.3 \times 10^5$ and then it rose again up to 0.45 in the supercritical zone. It is clear that the changes in the magnitude of the vortex shedding are related to the changes in the topology of the wake and the wake width. The reason why some investigators did not detect vortex shedding at $Re > 4 \times 10^5$ is not clear. However, at these Reynolds numbers the flow is quite unstable and aspects such as a low cylinder aspect ratio or vibrations in the wind tunnel can trigger three-dimensional effects in the wake and the loss of coherence in the vortex shedding. Indeed, [18] observed these effects for low aspect ratio cylinders and thus no regular signal where detected.

4 CONCLUDING REMARKS

Large eddy simulations of the flow past a circular cylinder at critical and supercritical Reynolds numbers have been carried out. The main flow parameters have been computed with reasonable agreement with experimental measurements. The presence of a laminar separation bubble on one side or both side of the cylinder surface depending on the Reynolds number has been detected. The turbulent shear-stresses just after separation

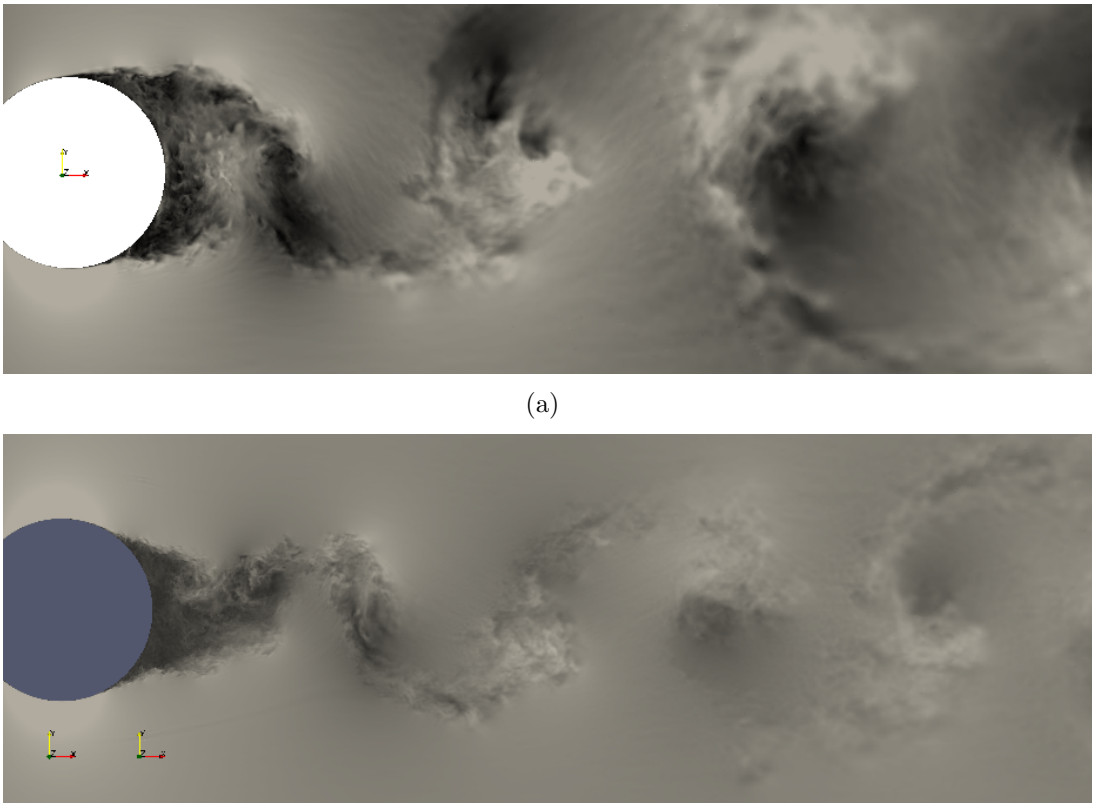

(a)

(b)

Figure 2: Instantaneous velocity profile at different Reynolds numbers (a) $Re = 2.5 \times 10^5$, (b) $Re = 7.2 \times 10^5$

of the boundary layer cause the transport of the momentum in the separated shear layer and are responsible for the closure of the laminar separation bubble. Vortex shedding has been detected at all Reynolds numbers, but the frequency at which vortices are shed increases as the flow transition from critical to supercritical regimes.

ACKNOWLEDGMENTS

This work has been by financially supported by the Ministerio de Economía y Competitividad, Secretaría de Estado de Investigación, Desarrollo e Innovación, Spain (ref. ENE2009-07689) and by the Collaboration Project between Universidad Politècnica de Catalunya and Termo Fluids S.L. We acknowledge PRACE for awarding us access to resource MareNostrum III based in Barcelona (Spain) through DRAGON project.

REFERENCES

[1] A. Roshko. Experiments on the flow past a circular cylinder at very high Reynolds number. *Journal of Fluid Mechanics*, 10(03):345–356, March 1961.

[2] M.S. Bloor. The transition to turbulence in the wake of a circular cylinder. *Journal of Fluid Mechanics*, 19(02):290–304, 1964.

[3] X. Ma, G.S. Karamanos, and G.E. Karniadakis. Dynamics and low-dimensionality of a turbulent wake. *J. Fluid Mechanics*, 410:29–65, 2000.

[4] O. Lehmkuhl, I. Rodríguez, R. Borrell, and A. Oliva. Low-frequency unsteadiness in the vortex formation region of a circular cylinder. *Physics of Fluids*, 25:085109, 2013.

[5] C. H. K. Williamson. Vortex Dynamics in the Cylinder Wake. *Annual Review of Fluid Mechanics*, 28(1):477–539, 1996.

[6] A. Prasad and C. H. K. Williamson. The instability of the separated shear layer from a bluff body. *Physics of Fluids*, 8:1347, 1996.

[7] P. W. Bearman. Investigation of the flow behind a two-dimensional model with a blunt trailing edge and fitted with splitter plates. *Journal of Fluid Mechanics*, 21:241–255, 1965.

[8] G Schewe. On the force fluctuations acting on a circular cylinder in crossflow from subcritical up to transcritical Reynolds numbers. *Journal of Fluid Mechanics*, 133:265–285, 1983.

[9] WJ Bursnall and L.K. Jr Loftin. Experimental investigation of the pressure distribution about a yawed circular cylinder in the critical Reynolds number range. Technical Report NACA TN2463, NACA, 1951.

[10] PW Bearman. On vortex shedding from a circular cylinder in the critical Reynolds number regime. *J. Fluid Mech*, 37:577–585, 1969.

[11] W.C.L. Shih, C. Wang, D. Coles, and A. Roshko. Experiments on flow past rough circular cylinders at large Reynolds numbers. *Journal of Wind Engineering and ...*, 49:351–368, 1993.

[12] F. Nicoud and F. Ducros. Subgrid-scale stress modelling based on the square of the velocity gradient tensor. *Flow, Turbulence and Combustion*, 62:183–200, 1999.

[13] Verzicco R. and R. Camussi. Numerical experimenrs on strongly turbulent thermal convection in a slender cylindrical cell. *Journal of Fluid Mechanics*, 477:19–49, 2003.

[14] F.X. Trias and O. Lehmkuhl. A self-adaptive strategy for the time integration of Navier-Stokes equations. *Numerical Heat Transfer. Part B*, 60(2):116–134, 2011.

[15] I. Rodríguez, R. Borrell, O. Lehmkuhl, C.D. Pérez-Segarra, and A. Oliva. Direct Numerical Simulation of the Flow Over a Sphere at Re = 3700. *Journal of Fluid Mechanics*, 679:263–287, 2011.

[16] I. Rodríguez, O. Lehmkuhl, R. Borrell, and A. Oliva. Flow dynamics in the wake of a sphere at sub-critical Reynolds numbers. *Computers & Fluids*, 80:233–243, 2013.

[17] O. Lehmkuhl, I. Rodríguez, A. Baez, A. Oliva, and C.D. Pérez-Segarra. On the large-eddy simulations for the flow around aerodynamic profiles using unstructured grids. *Computers&Fluids*, 84:176–189, 2013.

[18] E. Achenbach and E. Heinecke. On vortex shedding from smooth and rough cylinders in the range of Reynolds numbers 6e3 to 5e6. *J. Fluid Mech*, 109:239–251, 1981.